Electronic Supplementary Material (ESI) for Journal of Materials Chemistry A.

Supporting Information

I - Synthesis of Ti_3AlC_2 and Ti_2AlC MAX phases

$Ti_{n+1}AlC_n$ (n=1 or 2) MAX phases were synthesized using a conventional powder metallurgy technique. Titanium (-200 mesh, 99,95%, Alfa Aesar Karlsruhe Germany), titanium carbide TiC (4µm, 99,5%, Alfa Aesar) and aluminum (60-100 mesh 99,8%, Alfa Aesar) were used as starting materials. The powders were weighted according to the desired composition (Ti_2AlC and Ti_3AlC_2) except for Al which was introduced with a 10 wt% excess in order to compensate its loss by evaporation during the sintering process. After mixing for 30 min (Turbula Shaker Mixer), a homogeneous mixture without agglomerates is obtained. This mixture was then packed into a glass tube sealed under vacuum.

The sintering has been performed in a Nabertherm furnace under argon atmosphere for 2 h at 1450°C for both Ti_3AlC_2 and Ti_2AlC syntheses. Finally, the powders were sieved in order to select MAX phases with grain sizes lower than 25µm.

II - Influence of drying time on Ti_3C_2-Fe

XRD patterns at low angles of Ti_3C_2-Fe after drying at 80°C for different times are reported on Fig. S1. As observed, several (002) reflection peaks of MXenes are observed corresponding to different values of c parameter. With the increase of drying time, the peaks corresponding to the greatest c tend to disappear. This confirms that the greatest c are due to the presence of interlayer water. Moreover, this result shows the coexistence of structures having contrasted layer-to-layer distances (several (002) reflection peaks on a same XRD pattern) and that the removal of water is gradual at 80°C. This phenomenon was previously highlighted at ambient temperature with different relative humidity on Ti_3C_2 intercalated with cations [M. Ghidiu et al., *Chem. Mater.*, 2016, **28**, 3507–3514].

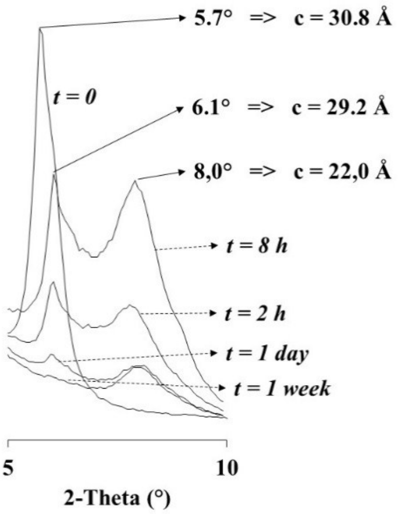

Fig. S1 XRD patterns of Ti_3C_2-Fe for different times of drying at 80°C.

III - Influence of immersion in water on the MXenes structure

The stability of the different MXene samples into water was investigated. The washing into deaerated water for 1 week involves the elimination of aluminum for all samples as discussed in the manuscript (ICP-OES - table 1). No significant modification on Ti_3C_2-Fe, except for the removal of $AlF_3.3H_2O$, is evidenced from XRD (Fig. S2a and b). Nevertheless, the formation of TiO_2 rutile (card n°98-000-9161 of the ICDD database) cannot be totally excluded since a peak with a very low intensity at 54.3° is observed (Fig S2b - Ti_3C_2-Fe-d) which potentially corresponds to the (121) diffraction peak of TiO_2 rutile (the most intense diffraction peak of TiO_2 rutile at 27.4 is overlapped with the (006) diffraction peak of the MXene, complicating the indexation). In a similar way, the XRD pattern of Ti_3C_2-Li-d does not show any significant modification after 1 week into deaerated water (Fig. S2c and d). Nevertheless, because of the previously mentioned overlap between the XRD peaks, the presence of TiO_2 rutile cannot be totally excluded. Similarly TiO_2 anatase (card n°98-000-9853 of the ICDD database) cannot be totally excluded since a broad peak with a very low intensity at 25.3° (which potentially corresponds to (110) diffraction peak of the TiO_2 anatase) is observed. For Ti_3C_2-HF-d, the loss of $TiOF_2$ is evidenced by XRD (Fig. S2 e and f). A broad peak with very low intensity at 25.2° attributed to TiO_2 anatase is hardly observed. This phase is probably formed from $TiOF_2$, unstable into water.

In brief, whatever the MXene, no significant oxidation phenomenon is clearly evidenced by XRD even after 1 week into deaerated water confirming the discussion in the manuscript based on EDS, Raman spectroscopy and S_{BET} results.

In contrast, broad diffraction peaks of TiO_2 anatase and/or rutile are observed on sample washed into deionized water with intensity increasing with the duration of the washing step (Fig. S2). Thus, this oxidation of the MXenes is due to oxygen dissolved into water.

For Ti_3C_2-Fe, the major formation of TiO_2 anatase is clearly evidenced after 1 week with the main (011) peak at 25.3° and the (020), (015) and (121) diffraction peaks at 47.9, 53.8 and 54.9° respectively. Nevertheless, a minor formation of rutile is likely (main peak of rutile close to 006 diffraction peak of MXene).

For Ti_3C_2-Li, no oxidation is clearly evidenced after 52h into deionized water by XRD. Nevertheless, as described in the manuscript, the oxidation phenomenon with the formation of TiO_2 anatase is evidenced by TEM. The non-observation of this phase by XRD is due to the probable low rate of oxidation. After one week (168h), the major formation of TiO_2 rutile is clearly evidenced by XRD with the (110), (121) and (220) diffraction peaks at 27.4, 54.3 and 56.6° respectively but the presence of TiO_2 anatase cannot be totally excluded since a peak with a very low intensity at 25.3° is observed.

For Ti_3C_2-HF, an intermediate behavior with the formation of rutile and anatase after 1 week is observed by XRD (Fig. S2).

These phase analyses by XRD combined with EDS, S_{BET}, TEM, Raman spectroscopy and XPS results confirm the discussion in the manuscript about the different reactivity versus water depending on the etchant.

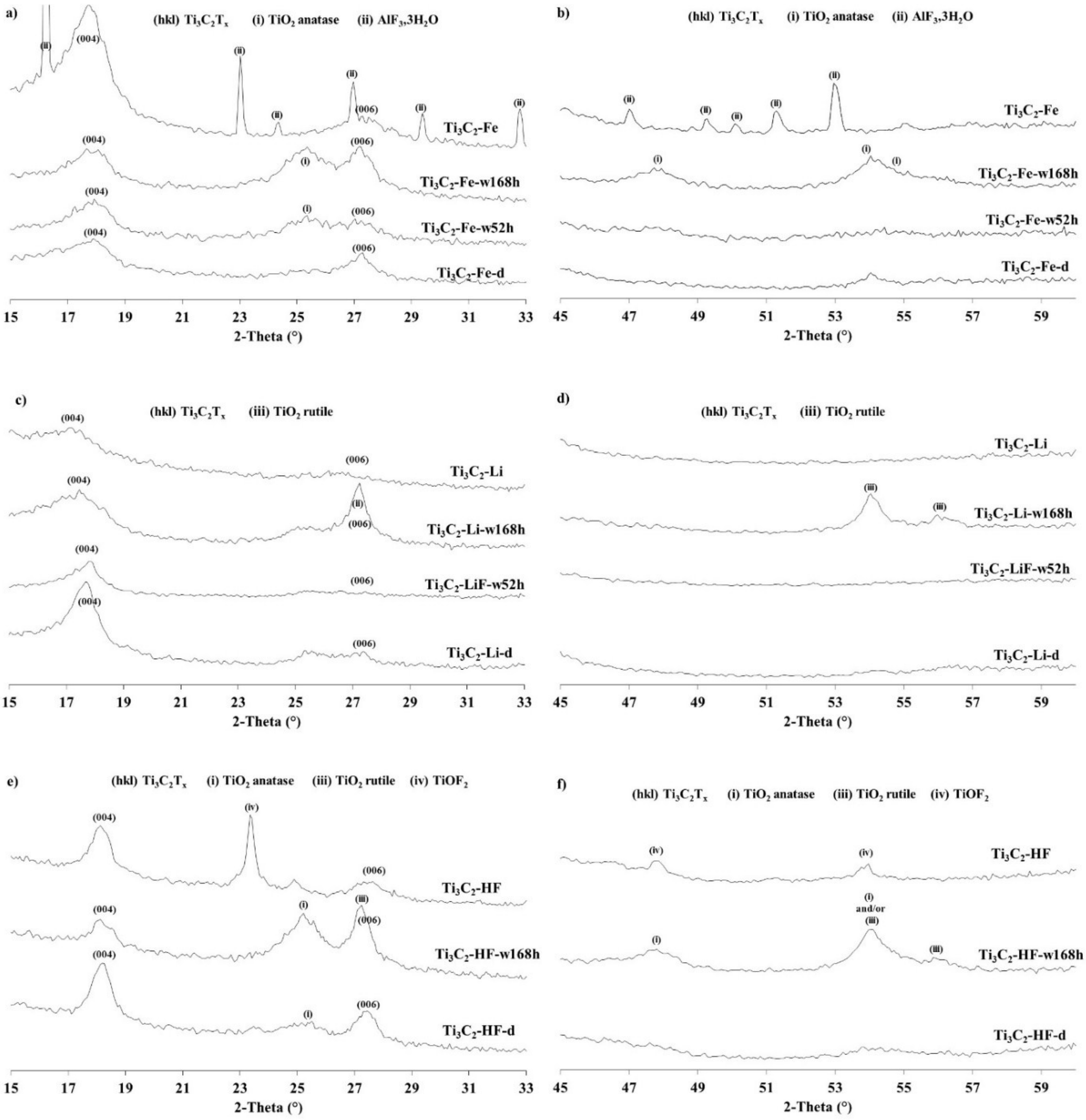

Fig. S2 XRD patterns before and after washing into deaerated (d) or deionized (w) water of Ti_3C_2-Fe (a and b), Ti_3C_2-Li (c and d) and Ti_3C_2-HF (e and f).

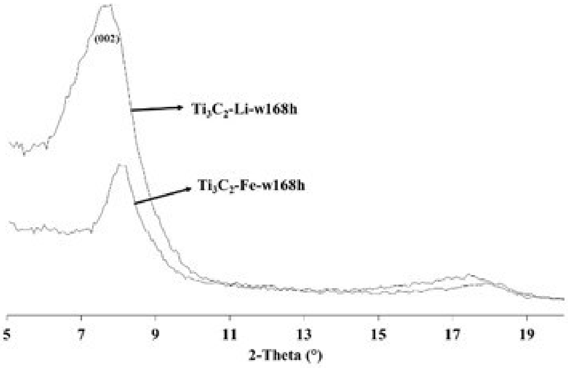

Fig. S3 XRD patterns (recorded in the same conditions) of Ti_3C_2-Fe-w168h and Ti_3C_2-Li-w168h in the (002) peak region.

IV - SEM results of Ti_3C_2-Fe

Fig. S4 shows a typical SEM micrograph of the Ti_3C_2-Fe sample with low magnification highlighting the aluminum rich rod-like structures. From EDS measurements performed on the rods, F/Al atomic ratios between 3 and 5 were determined indicating that these rods correspond probably to the aluminum fluoride (F/Al theoretical atomic ratio = 3) observed by XRD. On the isolated MXene sheets, very few amount of aluminum was detected (<0.05 atom of Al for 3 atom of Ti) showing that aluminum observed in the global sample (Ti/Al atomic ratio = 3/0.55 determined by ICP-OES) is located mainly on the rods and not in the sheets.

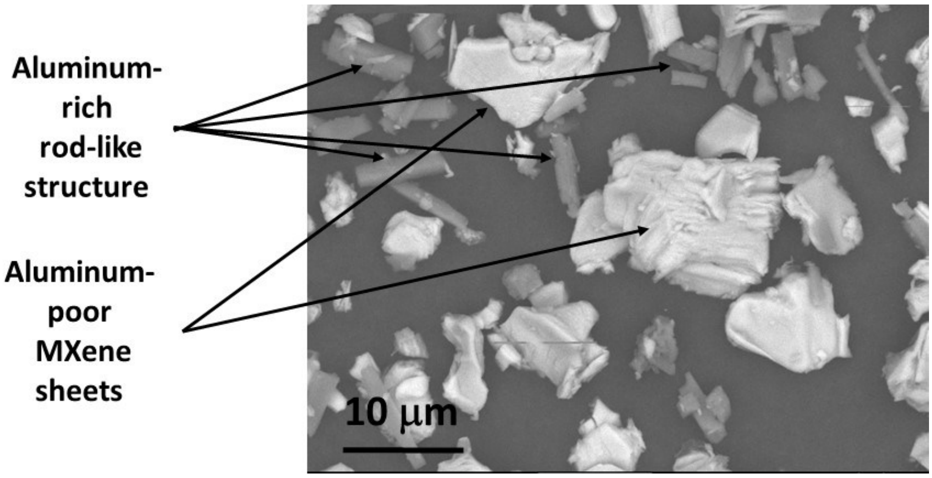

Fig. S4 Typical SEM micrograph of Ti_3C_2-Fe with low magnification

Fig. S5 shows a typical EDS spectrum of the Ti_3C_2-Fe sample showing the presence of iron. The Fe content is 0.08 for 3 Ti on average (estimated on 20 grains) with strong inhomogeneities from one grain to another (from 0 to 0.2).

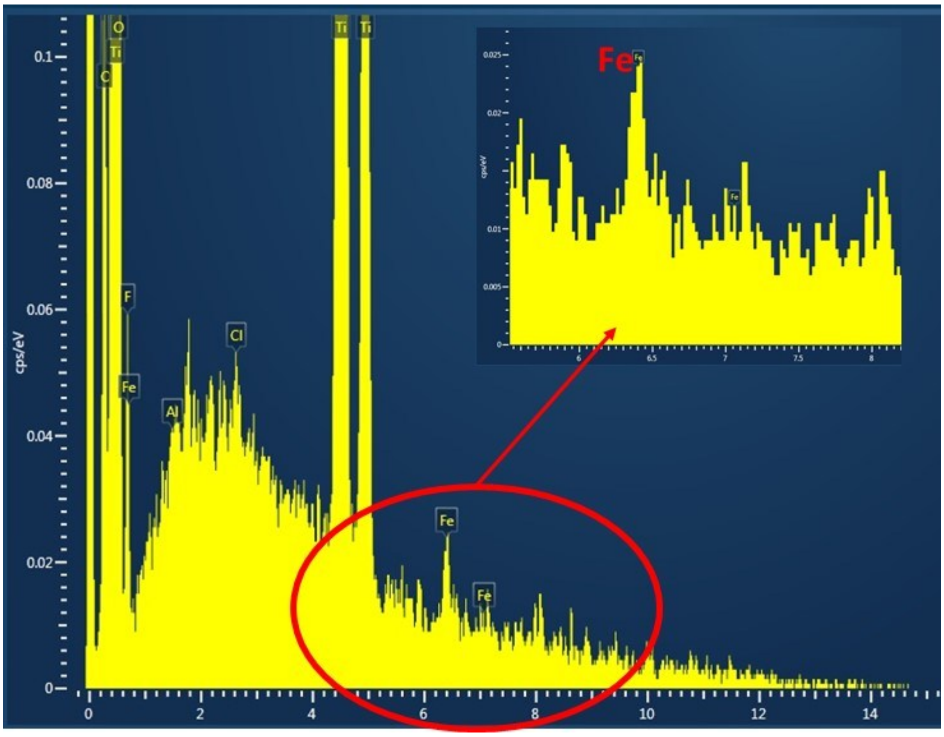

Fig. S5 Typical EDS spectrum (Aztec software) of isolated Ti_3C_2-Fe grain (Fig 3d of the manuscript)

V - Optical microscopy and AFM results

Atomic Force Microscopy was performed using a Dimension 3100 from Digital Instruments on tapping mode. A standard flattening procedure using WSxM software [I. Horcas et al., *Review of Scientific Instruments.*, 2007, **78,** 013705] was then performed to ensure flatness of the substrate and correct flake-to-substrate step height extraction. Few-microns laterally averaged altitude of the flake and the substrate were them compared, ensuring a step height uncertainty of 0.5 nm despite sample roughness. Optical Microscopy images were taken with an Optiphot-2 from Nikon, by reflection, using unpolarized white light from a halogen lamp, with a x40 objective and x10 ocular lenses, and acquired by a digital camera. Optical contrast between the otherwise almost transparent MXene flake and the substrate is made possible thanks to Fabry-Perot-like interference effect through the 250nm thick oxide layer [A. Miranda et al., *Mater. Res. Lett.*, 2017, **5,** 322-328].

Fig. S6 shows the typical optical microscopy and AFM images of the Ti_3C_2-Fe sample evidencing several micron large flakes. The AFM height profile is also presented. To isolate the flakes from the multilayered MXenes, the following protocol was used: after synthesis, the solution containing the Ti_3C_2-Fe MXene was centrifuged to separate the powders from the acid medium. After several washing steps with deionized water until the pH of the supernatant reached 6, the colloidal suspension in the supernatant was collected after a final centrifugation at 3500 rpm and deposited onto a silicium wafer covered by 250 nm of thermally-grown silicon dioxide by drop-casting. On figure S6, the step height of the MXene flake compared to the substrate was measured to be 13.9 nm. As XRD measurements on the Ti_3C_2-Fe powders indicate a c-parameter of 2.2 nm, this thickness corresponds roughly to 13.9/(c/2) = 12.6 layers of Ti_3C_2. However, the MXene flakes measured by AFM are obtained from a colloidal solution without specific drying procedure: this may lead to intercalation of water between the layers, inducing a larger c-parameter than the one obtained on the dried powders (fig 2 – c = 2.7 nm). In addition, AFM includes an offset due to water intercalation below the flake. For these reasons, the number of layers of the 13.9 nm-thick MXene is probably smaller than the evaluation above, typically from 8 to 10 layers.

The height of the different observed flakes is between 10 and 17 nm corresponding approximatively to 7-13 layers. This delamination protocol is not optimized yet and, based on the works of the literature [C. J. Zhang et al, *Chem. Mater.*, 2017, **29,** 4848-4856], we can reasonably expect to isolate thinner flakes or mono-layer flakes.

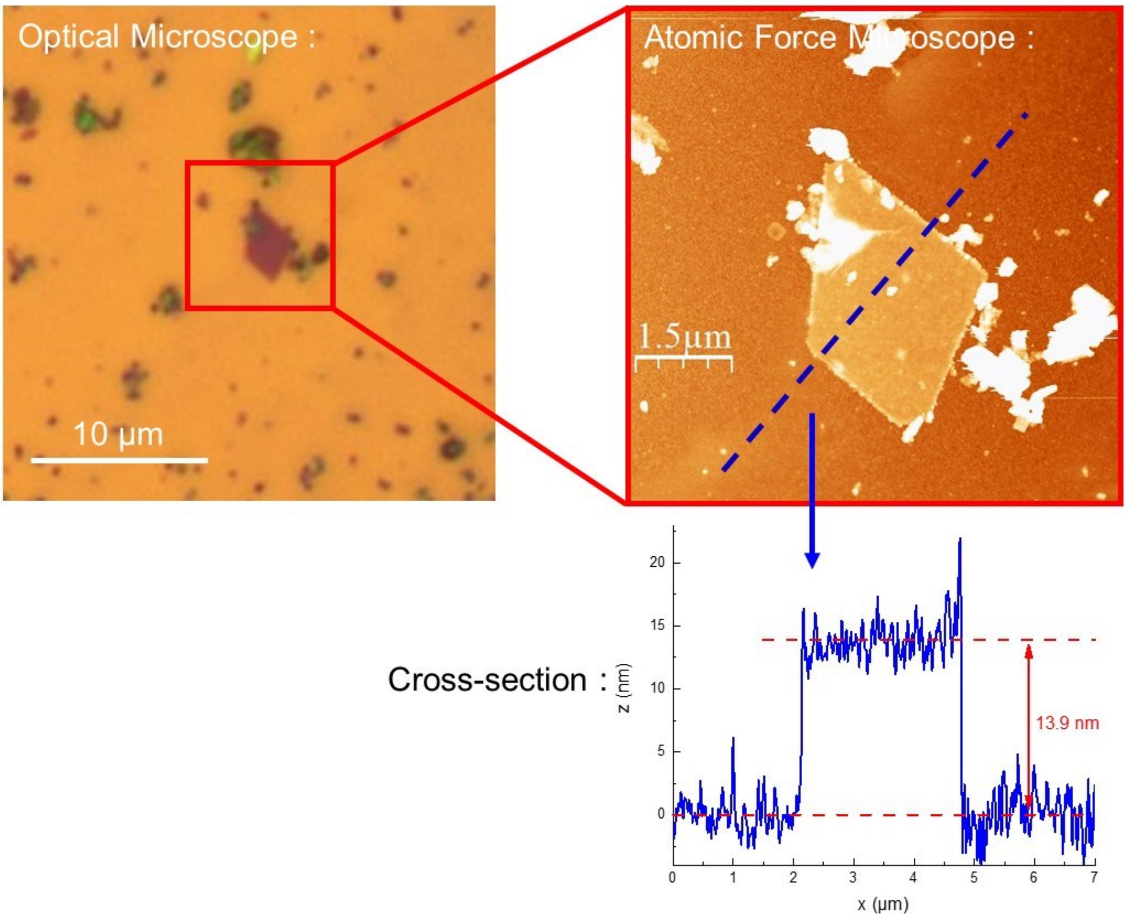

Fig. S6 Typical optical microscope and AFM images of delaminated Ti_3C_2-Fe grain with the corresponding height profile

VI - Role of aluminum salts and iron on the oxidation of the MXenes

As discussed in the manuscript, a high amount of AlF_3 is obtained with the FeF_3/HCl etching method in comparison with the LiF/HCl (table 1 and S1). The presence of this salt can potentially play a role in the oxidation of the MXene. Several experiments were performed to highlight the role of both this salt and the iron intercalated in the MXene layers. Instead of direct filtration of the mixture after exfoliation following by washing with water as described in the experimental part, the samples was washed with HCl 6M (3 times) and deionized water (3 times) by centrifugation before filtration. The samples are referred as to Ti_3C_2-M-HCl (with M = Fe or Li in function of the etching agent) and then immerged in deionized water during 168h. Experiments of immersion into deionized water were also performed on samples which are preliminary washed in deaerated water after synthesis during 5h and referred as to Ti_3C_2-M-d5h. The combination of the 2 steps (washing with HCl and deaerated water) was also performed and the corresponding samples are referred as to Ti_3C_2-M-HCl-d5h.

As observed on table S1, the aluminum content cannot be removed by the washing step with HCl even if the amount slightly decrease. Although this method is often used in the literature to remove the salt impurities from MXenes [M. Ghidiu et al, *Chem. Mater.*, 2016, **28,** 3507-3514], it failed in our case. This can be explained by 2 reasons: the dissolution of aluminum fluoride salts is probably kinetically limited and the washing time by HCl is short (5 min each) and/or the concentration is too high (0.5 g of powder for 40 mL of HCl 6M) avoiding the complete dissolution of the Al salt. In contrast, this step leads to the total removal of the iron atoms, probably by exchange of Fe^{n+} by H^+ between the MXenes layers. For the complete removal of aluminum, a simple step of washing in deaerated water during 5h at low concentration (0.6 g of powder for 350 mL of deaerated water) is adequate (Ti_3C_2-Fe-d5h – table S1) allowing to retain the iron content. A combination of both steps lead to the complete removal of aluminum and iron (Ti_3C_2-Fe-HCl-d5h – table S1). This evolution of the aluminum content depending on the washing step is also observed for Ti_3C_2 prepared from the LiF/HCl etching agent (table S1). The formation of the MXene without TiO_2 peaks is observed by XRD whatever the washing step and etching method used.

On the different samples prepared from FeF_3/HCl and after immersion into deionized water for 168h, a mixture of TiO_2 anatase and rutile phases with the MXenes are observed. Nevertheless, even if the XRD quantification is difficult from these patterns, the anatase/rutile ratio evolves clearly as observed from the intensity of the XRD peaks (fig 12 of the manuscript). Indeed, the fraction of rutile increases with the removal of aluminum and/or iron (Ti_3C_2-Fe-HCl, Ti_3C_2-Fe-d5h, Ti_3C_2-Fe-HCl-d5h after immersion into water during 168h) in comparison with Ti_3C_2-Fe-w168h. Thus, the presence of both iron and aluminum in the sample inhibits partially the anatase to rutile phase transformation (AR-T). This is in agreement with the ref [D. A. H.

Hanaor et al, *J. Mater. Sci.*, 2011, **46,** 855-874] where Al is known to inhibit this transformation. In a similar way, the presence of weakly loaded Fe^{n+} (typically < 2 %), as in our case, also inhibits this transformation [D. A. H. Hanaor et al, *J. Mater. Sci.*, 2011, **46,** 855-874 and Q. Gao et al, *Dyes and Pigments*, 2012, **95,** 96-101]. Nevertheless, the presence of TiO_2 anatase is always observed on each sample, which is confirmed by Raman spectroscopy with spectra similar to Ti_3C_2-Fe-w168h spectrum (fig 8).

Whatever the washing step, only the rutile phase is clearly observed by XRD on the sample prepared from LiF/HCl and the XRD pattern is equivalent to Ti_3C_2-Li-w168h of the Figure S2. These results confirm that the LiF/HCl method promotes the rutile formation after 168h of treatment even if aluminum is totally removed which is confirmed by Raman spectroscopy where only the spectral signature of the MXene is clearly observed as in the case of Ti_3C_2-Li and Ti_3C_2-Li-w168h (figure 8). Contrary to Fe^{n+} in low concentration and Al^{3+}, Li^+ is known to be in favour of AR-T [D. A. H. Hanaor et al, *J. Mater. Sci.*, 2011, **46,** 855-874].

The stability in deionized water for 168h of Ti_3C_2-Li was also studied in the presence of dissolved AlF_3. For this experiment, 0.5 Al for 3 Ti was added to obtain a Ti/Al ratio similar to that of the Ti_3C_2-Fe samples. The obtained XRD pattern and the Raman spectrum are similar to those obtained for Ti_3C_2-Li-w168h, showing the minor role of aluminum on the rate of oxidation as well as on the promotion or inhibition of TiO_2 anatase for this sample, the role of the lithium (or the rate of oxidation, see below) being probably more important.

Finally, whatever the early washing steps used, after immersion in water during 168h, the MXenes prepared from FeF_3/HCl is more oxidized than the MXenes prepared from LiF/HCl since the 002 peak of Ti_3C_2 is systematically much less intense as observed on fig S3. Moreover, Raman spectra of Fe-based MXenes correspond to TiO_2 anatase with no or small spectral signature of the MXene unlike LiF/HCl showing systematically the signature of the MXene as shown on fig 8 on Ti_3C_2-M-w168h samples (the presence of a

weak amount of rutile being difficult to observe by Raman spectroscopy as discussed in the manuscript). Thus, the role of the oxidation rate in the anatase/rutile selectivity can not be excluded, a high rate favoring potentially the anatase formation.

Table S1 ICP-OES and XRD analyses of different MXenes before and after immersion into deionized water during 168h. The content of each element is rationalized to 3 titanium atom

	Before deionized water			**After deionized water**			
	Ti	**Al**	**Fe**	**Ti**	**Al**	**Fe**	**XRD of TiO_2**
Ti_3C_2-Fe	3	0.51	0.07	3	0.02	0.07	Anatase (+ rutile)
Ti_3C_2-Fe-HCl	3	0.37	0	3	0.01	0	Anatase + rutile
Ti_3C_2-Fe-d5h	3	0.02	0.06	3	0.02	0.06	Anatase + rutile
Ti_3C_2-Fe-HCl-d5h	3	0.03	0	3	0.01	0	Anatase + rutile
Ti_3C_2-Li	3	0.10	-	3	0.01	-	rutile
Ti_3C_2-Li-HCl	3	0.08	-	3	0.01	-	rutile
Ti_3C_2-Li-d5h	3	0.02	-	3	0.01	-	rutile
Ti_3C_2-Li-HCl-d5h	3	0.02	-	3	0.02	-	rutile

VII - Influence of the duration of immersion in deionized water of Ti_3C_2-Fe

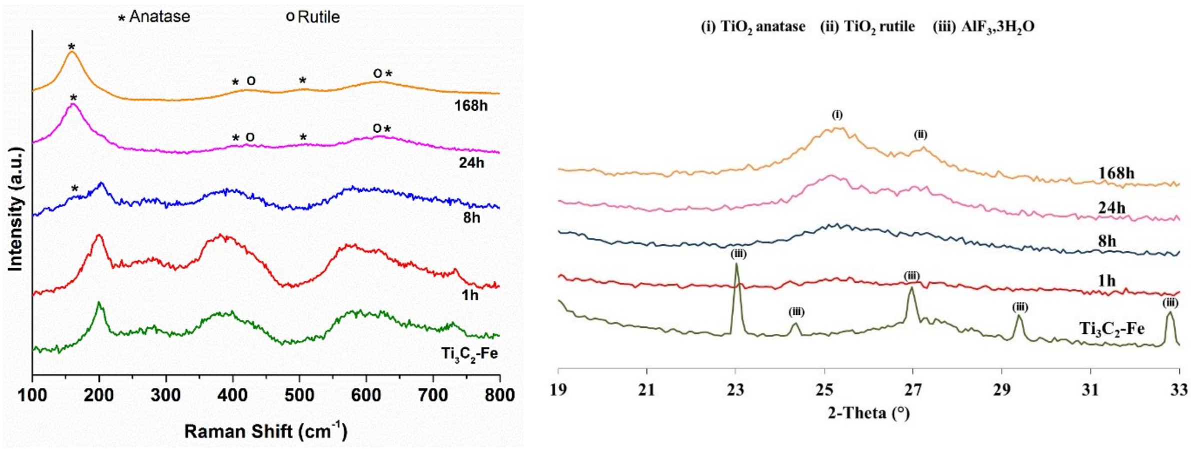

Fig. S7 (left) Raman spectra and (right) XRD patterns of as-synthesized Ti_3C_2-Fe and after immersion in deionized water for 1h, 8h, 24h and 168h.